



Project no.043386

TRIGS

TRIGGERING INSTABILITIES IN MATERIALS AND GEOSYSTEMS

Sixth Framework Programme (FP6) - STREP

New and Emerging Science and Technology Pathfinder (NEST)

Deliverable no. 1.5.2 Synthesis report on failure of layered materials

Due date of deliverable: 01 Jan 2010

Actual submission date: 22 Jan 2010

Start date of project: 1 January 2007

Duration: 36 month

Organisation name of lead contractor for this deliverable: WSL/SLF

Diffusion Level: PU

Report on measurements methods to study failure of layered materials

I. Reiweger and J. Schweizer

WSL Institute for Snow and Avalanche Research SLF, Davos, Switzerland

Introduction

Dry-snow slab avalanches start with a failure in a weak snow layer below a cohesive slab of ample thickness (e.g. Schweizer et al., 2003). If the initial failure reaches a sufficiently large size and the snowpack conditions are favourable for crack propagation, the initial crack can propagate and an avalanche may release. While the formation of the initial failure is well understood and documented in the case of artificially triggered dry-snow slab avalanches (e.g. van Herwijnen and Jamieson, 2005), the initiation process for spontaneous dry-snow slab avalanches remains unclear.

Field measurements of the strength of weak snow layers, or snow layers in general, exhibit large scatter (Föhn et al., 1998; Jamieson and Johnston, 2001). This is mainly because the mechanical properties of snow depend on microstructural characteristics which are variable both in space and time. This impairs the reproducibility of experiments performed at different times even at the same snowpack location.

Various studies on shear failure of homogeneous snow samples under controlled laboratory conditions have therefore been performed (e.g. Schweizer, 1998). Depending on snow type and temperature these studies typically show brittle behaviour of snow at strain rates faster than about 10^{-3} s^{-1} and ductile behaviour at smaller strain rates. In order to quantify the small scale (microscopic) failure processes taking place in the snow before catastrophic (or macroscopic) failure, it has been tried to measure acoustic emissions during compression tests (Scapozza et al., 2004) and displacement-controlled shear experiments (McClung, 1987). We measure acoustic emissions in load controlled shear experiments, using the same acoustic setup as Scapozza et al. (2004).

We present preliminary results from shear experiments performed with a newly designed shear apparatus with both natural and artificially produced homogeneous and layered snow samples. With these experiments we aim to understand the mechanical response of the snow samples to loading and the mechanisms which lead to catastrophic failure of the samples. The catastrophic failure of a snow sample in the lab is assumed to correspond to the initial failure which leads to crack propagation and subsequently to dry-snow slab avalanche release in the field.

Methods

Snow samples

Homogeneous snow samples can either be taken from the field or produced in the laboratory. For artificial low and medium density snow samples (density $\rho < 400 \text{ kg m}^{-3}$) we took new snow produced by a snow machine (Meier, 2006), sieved it into a box, compressed it, and let it sinter for hours or days, depending how hard and dense we wanted the sample. For high density snow, it was sufficient to take grounded ice instead of new snow; after a few hours of sintering the structure of the sieved sample equalled the structure of natural high density snow (rounded grains).

Considering avalanche release, snow samples containing a weak layer (either buried surface hoar or

depth hoar) are more relevant than homogeneous snow samples. Such layered samples can again either be harvested in the field or produced in the cold laboratory.

In the cold lab, depth hoar was grown by applying a strong vertical temperature gradient to a snow sample, as has first been described by Fukuzawa and Narita (1993) who grew depth hoar on the surface of a snow sample. Our snow samples consisted of a layer of low density snow (snowflakes produced by the snow machine) sandwiched between two dense snow layers ($\rho = 300 \text{ kg m}^{-3}$) (produced by sieving grounded ice). A heat foil placed at the bottom of the layered snow sample was used to create a temperature gradient of about 150 K m^{-1} . Within two to three days the low-density layer transformed into depth hoar. We also produced layers of surface hoar by letting water vapour freeze on a cold snow surface thereby mimicking the natural process of surface hoar formation. The created surface hoar crystals were then covered with new snow produced by the snow machine. Figure 2 schematically shows the experimental setups.

Shear experiments

A newly designed force-controlled shear apparatus (Fig. 2) was developed to load snow samples under conditions similar to those in a natural snowpack. The typical size of the snow samples that can be tested with the apparatus is $0.2 \text{ m} \times 0.1 \text{ m} \times 0.05 \text{ m}$. Prior to loading, the snow sample was placed between two sample holders, i.e. the bottom plate and the upper sample holder, and tilted by an angle α . The snow sample was then gradually loaded by increasing the weight on the upper sample holder. This was achieved by draining fluid (i.e. alcohol) from a container placed on top of the shear apparatus into a container placed below the snow sample and attached to the top sample holder. The loading rate can be varied from 0.01 N s^{-1} representing snowfall) to 3 N s^{-1} (representing rapid loading).

The tilt angle α , similar to slope angle in the field, can be varied and with it the ratio of normal to shear force. The force acting on the sample, i.e. the weight of the drained liquid, was recorded with a force sensor positioned below the snow sample. The displacements of the upper sample holder, in the slope parallel and slope normal direction, were measured with displacement sensors.

The displacement field within the snow sample was visualized with a particle image velocimetry algorithm (PIV). The algorithm recognized patterns on an image taken from the snow sample and tracked it over various images. By comparing a sequence of images taken at different times during the experiment, the

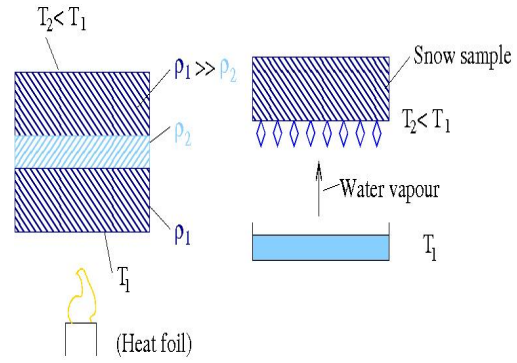


Figure 1: Experimental setup for producing a layer of faceted crystals (left) and surface hoar (right). T denotes temperature and ρ denotes density.

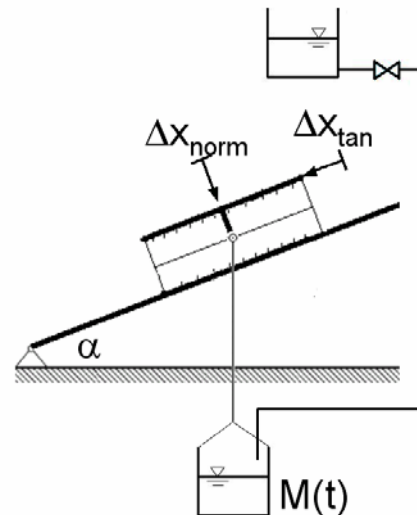


Figure 2: Schematic of the new force-controlled shear apparatus. α denotes the slope angle, M is the mass in the container (dependent on time), and x_{norm} and x_{tan} denote the normal and tangential (shear) displacement of the upper plate.

displacement, deformation, and path lines can be calculated. Additionally, acoustic emission signals during the shear experiments were recorded with piezoelectric transducers which were mounted in the bottom plate of the sample holder.

RESULTS AND DISCUSSION

Figure 3 shows typical force and displacement curves during a shear experiment with a layered snow sample (length: 9 cm; width: 7 cm; lower layer height: 3.4 cm; grain type: faceted crystals; grain size: 1 mm; hardness: pencil; weak layer: height 0.1 cm; grain type: surface hoar; grain size: 1 mm; hardness: fist; upper layer: height 3.8 cm; grain type: rounded grains; grain size: 0.5 mm; hardness: pencil). The sample failed catastrophically at $t = 368$ s. Even though the sample was loaded at a constant rate of 0.15 N s^{-1} , the deformation rate did not increase linearly up to failure, but the sample progressively weakened.

The displacement field derived with PIV of two photographs taken at $t = 356$ s and $t = 366$ s (i.e. shortly before fracture) during the same experiment is shown in Figure 4. Clearly, the deformation was concentrated within the weak layer. This has often been assumed but has not been documented so far.

Figure 5 shows typical results of acoustic emissions recorded during an experiment where a homogeneous snow sample ($\rho = 400 \text{ kg m}^{-3}$, $\alpha = 30^\circ$) was gradually loaded; no fracture occurred. Initially, for 42 s, the loading rate was constant (3.25 N s^{-1}). Then it decreased (as the top container emptied) until the final load of 160 N was reached. There was an initial compression of the snow sample at the beginning of the loading process of 0.5 mm (dark grey curve in Fig. 5a). Thereafter, no further compression of the sample was observed. The shear rate (light grey curve in Fig. 5a) slowly increased while the loading rate was constant and decreased as soon as the loading rate diminished.

As soon as the sample was loaded the acoustic emission count rate increased strongly until it reached a value of about $1000 \text{ counts s}^{-1}$ after 25 s (Fig. 5b). The count rate approximately stayed at this level for 20 s and decreased slowly afterwards. The AE sensor used in this experiment was resonant transducer (DECI SE9125-M) with a resonance frequency of 125 kHz.

The comparison of the count rate with the shear deformation is particularly interesting. So far all our measurements showed that a change in shear rate involved a change in count rate. Although the loading rate was constant (until the final load was reached) the shear deformation rate was not constant, indicating that different deformation processes were taking place within the snow sample. The coinciding change in acoustic emission rate indicates that the acoustic emission rate was related to the deformation/failure process within the material. After a period with a constant deformation rate, strain softening took place and the sample deformed faster under the same loading rate. This strain softening resulted in a drop in the count rate. Assuming that acoustic emission signals originated from breaking ice bonds, this would mean that in the case of constant deformation rate and constant count rate, the number of breaking ice bonds would be equal to the number of newly forming bonds. If on the other hand, the deformation rate increased and the count rate decreased, the material was in a state where the number of breaking bonds was not counterbalanced by the formation of new bonds, and hence the sample softened.

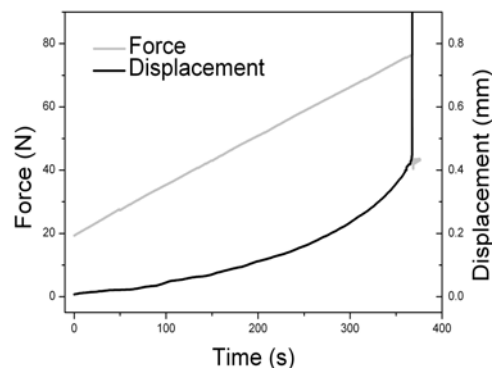


Figure 3: Force and slope parallel displacement during a shear experiment with a layered snow sample.

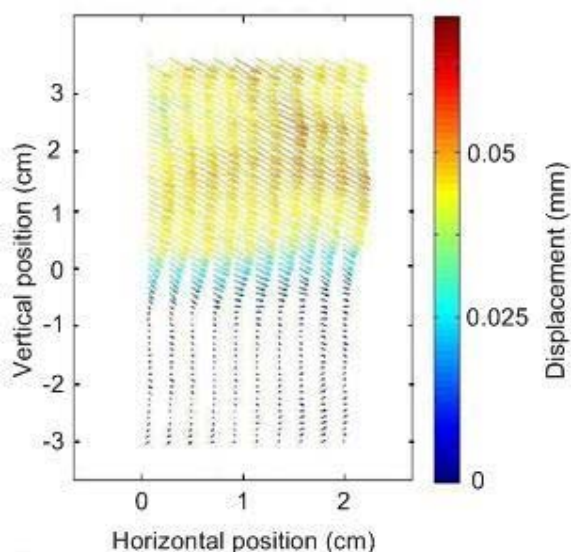


Figure 4: Displacement on the side of a layered snow sample during the force-controlled shear experiment shown in Fig. 3. The weak layer is located between -0.1 and 0 cm, and we can clearly see a displacement gradient (i.e. concentration of deformation) there.

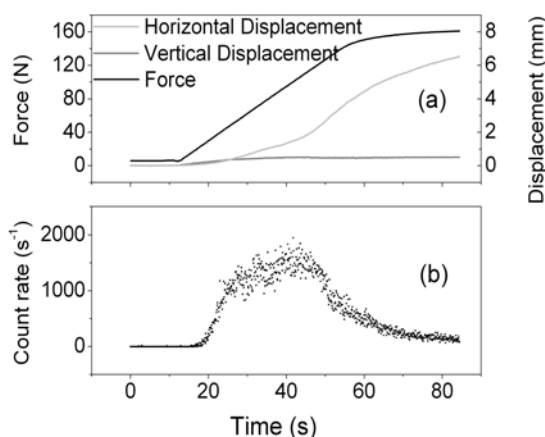


Figure 5: Load, displacement, and acoustic emissions (count rate) measured during a shear experiment with a homogeneous snow sample produced in the cold laboratory.

CONCLUSIONS AND OUTLOOK

We have measured the load, the global deformation, the deformation within the snow sample and acoustic emissions in a newly designed force-controlled shear apparatus. Results from PIV clearly showed that when a layered snow sample was subjected to a constant slow loading rate, the deformation was concentrated within the weak layer. Preliminary results of the acoustic emission measurements of the homogeneous samples indicated that the AE may hint on the micromechanics during deformation.

In the future, we will measure acoustic emissions during shear experiments with snow samples containing a weak snow layer, since this setup is most relevant for dry-snow slab avalanche release. The aim of these experiments will be to relate the acoustic emission measurements to the failure behaviour of the samples.

REFERENCES

Föhn, P.M.B, Camponovo, C. and Krüsi, G., 1998. Mechanical and structural properties of weak snow layers measured in situ. *Ann. Glaciol.*, 26: 1-6.

Fukuzawa, T. and Narita, H., 1993. An experimental study on the mechanical behavior of a depth hoar under shear stress, *Proceedings ISSW 1992, International Snow Science Workshop, Breckenridge, Colorado, U.S.A., 4-8 October 1992. Colorado Avalanche Information Center, Denver CO, U.S.A., pp. 171-175.*

Jamieson, B. and Johnston, C.D, 2001. Evaluation of the shear frame test for weak snowpack layers. *Ann. Glaciol.*, 32: 59-69.

- McClung, D.M., 1987. Mechanics of snow slab failure from a geotechnical perspective. In: B. Salm and H. Gubler (Editors), *Symposium at Davos 1986 - Avalanche Formation, Movement and Effects*, IAHS Publ., 162. International Association of Hydrological Sciences, Wallingford, Oxfordshire, U.K., pp. 475-508.
- Meier, M., 2006. *Produktion von naturidentischem Schnee*. M.Sc. Thesis, ETH Zurich, Switzerland, doi:10.3929/ethz-a-005674246.
- Scapozza, C., Bucher, F., Amann, P., Ammann, W.J. and Bartelt, P., 2004. The temperature- and density-dependent acoustic emission response of snow in monoaxial compression tests. *Ann. Glaciol.*, 38: 291-298.
- Schweizer, 1998. Laboratory experiments on shear failure of snow. *Ann. Glaciol.*, 26: 97-102.
- Schweizer, J., 1999. Review of dry snow slab avalanche release. *Cold Reg. Sci. Technol.*, 30(1-3): 43-57.
- Schweizer, J., Jamieson, B. and Schneebeli, M., 2003. Snow avalanche formation. *Rev. Geophys.*, 41(4): 1016.
- van Herwijnen, A. and Jamieson, B., 2005. High speed photography of fractures in weak snowpack layers. *Cold Reg. Sci. Technol.*, 43: 71-82.